Dopamine 2 Receptor Signaling Controls the Daily Burst in Phagocytic Activity in the Mouse Retinal Pigment Epithelium

Varunika Goyal,[1] Christopher DeVera,[1] Virginie Laurent,[2] Jana Sellers,[3] Micah A. Chrenek,[3] David Hicks,[2] Kenkichi Baba,[1] P. Michael Iuvone,[3,4] and Gianluca Tosini[1,3]

[1]Neuroscience Institute and Department of Pharmacology and Toxicology, Morehouse School of Medicine, Atlanta, Georgia, United States
[2]Institut des Neurosciences Cellulaires et Intégratives (INCI), Strasbourg, France
[3]Department of Ophthalmology and Emory Eye Center, Emory University, Atlanta, Georgia, United States
[4]Department of Pharmacology, Emory University, Atlanta, Georgia, United States

Correspondence: Gianluca Tosini, Neuroscience Institute and Department of Pharmacology and Toxicology, Morehouse School of Medicine, 720 Westview Drive, SW, Atlanta, GA 30310, USA; gtosini@msm.edu.

VG and CD contributed equally to this work.

Received: June 27, 2019
Accepted: March 25, 2020
Published: May 12, 2020

Citation: Goyal V, DeVera C, Laurent V, et al. Dopamine 2 receptor signaling controls the daily burst in phagocytic activity in the mouse retinal pigment epithelium. *Invest Ophthalmol Vis Sci.* 2020;61(5):10. https://doi.org/10.1167/iovs.61.5.10

Purpose. A burst in phagocytosis of spent photoreceptor outer fragments by RPE is a rhythmic process occurring 1 to 2 hours after the onset of light. This phenomenon is considered crucial for the health of the photoreceptors and RPE. We have recently reported that dopamine, via dopamine 2 receptor (D_2R), shifts the circadian rhythm in the RPE.

Methods. Here, we first investigated the impact of the removal of D_2R on the daily peak of phagocytosis by RPE and then we analyzed the function and morphology of retina and RPE in the absence of D_2R.

Results. D_2R knockout (KO) mice do not show a daily burst of phagocytic activity after the onset of light. RNA sequencing revealed a total of 394 differentially expressed genes (DEGs) between ZT 23 and ZT 1 in the control mice, whereas in D_2R KO mice, we detected 1054 DEGs. Pathway analysis of the gene expression data implicated integrin signaling to be one of the upregulated pathways in control but not in D_2R KO mice. Consistent with the gene expression data, phosphorylation of focal adhesion kinase (FAK) did not increase significantly in KO mice at ZT 1. No difference in retinal thickness, visual function, or morphology of RPE cells was observed between wild-type (WT) and D_2R KO mice at the age of 3 and 12 months.

Conclusions. Our data suggest that removal of D_2R prevents the burst of phagocytosis and a related increase in the phosphorylation of FAK after light onset. The pathway analysis points toward a putative role of D_2R in controlling integrin signaling, which is known to play an important role in the control of the daily burst of phagocytosis by the RPE. Our data also indicate that the absence of the burst of phagocytic activity in the early morning does not produce any apparent deleterious effect on the retina or RPE up to 1 year of age.

Keywords: dopamine, dopamine receptors, RPE, retina, circadian, phagocytosis

The RPE is a monolayer of cells that performs many vital functions for maintaining the health and physiology of retina. The RPE is involved in the daily phagocytosis of shed photoreceptor outer segments (POS).[1] Previous studies have shown that the process of RPE phagocytosis starts with shed photoreceptor outer segment interacting with integrin ligand MFG-E8.[2] The next steps comprise of engagement with $\alpha v\beta 5$ integrin receptors ($\alpha v\beta 5$[3,4]), activation of tyrosine kinases ($\alpha v\beta 5$-associated focal adhesion kinase [FAK]); cell surface receptor MerTK,[5,6] and re-localization of Rho family GTPase "Rac1" to recruit F-actin to phagocytic cups.[7] A recent genomic study in the mouse has also implicated phosphoinositide signaling in the regulation of the peak of phagocytic activity by the RPE.[8] Lack of phagocytosis by RPE leads to accumulation of POS debris in the subretinal space followed by photoreceptors degeneration in the rat[9] and mice.[10]

Further studies have also shown that the phagocytic activity of the RPE peaks in the morning, shortly after the onset of light (1–2 hours) in many different mammalian species.[11–14] This peak or burst in phagocytosis follows a circadian rhythm as the peak continues to occur even after the animals are kept in complete darkness.[11–14] Disruption in the daily peak of RPE phagocytosis impairs retinal and/or RPE functions because mice in which the $\alpha v\beta 5$ integrin receptor has been disabled by removing the gene *Itgb5*, which codes for the $\beta 5$ subunit of the receptor ($\beta 5^{-/-}$ mice), fail to show the morning burst of phagocytic activity. Moreover, during the aging process, $\beta 5^{-/-}$ mice also show a decrease in visual function (i.e. the amplitude of the a- and b-wave of the

scotopic ERG) and accumulate more lipofuscin in the RPE with respect to control mice.[4] Interestingly, it has also been reported that just a change in the timing of the peak in the phagocytic activity is associated with an increase in lipofuscin accumulation and photoreceptor loss during aging.[15] Finally, it was worth noting that the mechanism controlling this peak seems to be located within the RPE because the diurnal rhythm, in the exposure of phosphatidylserine by rod outer segments is not entirely controlled by the photoreceptors, but RPE cells participate in the synchronization of this process.[16]

Several lines of evidence suggest that dopamine (DA) is involved in the regulation of rhythmic RPE functions in vivo. For example, inhibition of DA synthesis during the early part of the light phase induced a significant reduction of disk shedding and phagocytosis[17] and mice whose dopaminergic neurons have been destroyed by 1-methyl-4-phenyl-1,2,3,6-tetrahydropyridine (MPTP) accumulate a large number of residual bodies in the RPE.[18] Besides, we have recently reported that a circadian clock is present in the RPE[19] and this clock is entrained to the external light-dark cycles by DA via dopamine 2 receptors (D_2R) that are present on the RPE.[20]

In this study, we first investigated the effect of D_2R removal on the daily burst of phagocytic activity and then we explored the effects that removal of these receptors may have on retinal and RPE morphology and function during aging.

Materials and Methods

Animals

D_2R ($Drd2^{tm1Low}$) knock-out (KO) and C57BL/6J (wild-type [WT]) mice, purchased from The Jackson Laboratory (Bar Harbor, ME, USA) and bred at Morehouse School of Medicine, were used in this study. Mice were maintained in 12 hours of light and 12 hours of dark with lights on (zeitgeber time [ZT] 0) at 06:00 AM and lights off (ZT 12) at 6:00 PM. Genotype of the mice was confirmed by PCR analysis of DNA samples prepared from tail tips by using the primers 5′-CACTCCGCCACTTGACATACA-3′ and 5′-TCTCCTCCGACACCTACCCCGA-3′. All experimental procedures were conducted in accordance with the National Institutes of Health (NIH) Guide on Care and Use of Laboratory Animals and were approved by the Morehouse School of Medicine Animal Care and Use Committee.

Phagosome Counting

Eyecups were fixed overnight in 4% paraformaldehyde at 4 degrees Celsius (°C), transferred to series of sucrose solutions (10%, 20%, and 30%, each for 2 hours) and embedded (Tissue-Tek; Sakura Fintek, Tokyo, Japan; #4583). Then 10-μm-thick cryostat sections were prepared and stored at −20°C until ready for use. The sections were permeabilized with Triton X-100 (0.1% in PBS for 5 minutes) and then saturated with PBS containing 0.1% BSA, 0.1% Tween-20, and 0.1% sodium azide (buffer A) for 30 minutes. Sections were incubated overnight at 4°C with primary antibody diluted in buffer A. The primary antibody used for this purpose was monoclonal anti-rhodopsin antibody Rhodopsin 4D2° (see Ref. 15 for details). Secondary antibody incubation was performed at room temperature for 2 hours with Alexa (488 nm) goat anti-rabbit (Thromofischer Scientific, Santa Clara, CA, USA; #R37116). Cell nuclei were stained with 4,6-diamino-phenyl-indolamine (DAPI; Invitrogen, Carlsbad, CA, USA; #D1306). Slides were washed thoroughly, mounted in PBS and glycerol (1:1), and observed with a confocal laser scanning microscope (LSM 700 version 2.5; Carl Zeiss Meditec, Jena, Germany).[15]

Library Preparation for RNA-Sequence

Eyes were obtained from WT and D_2R KO mice at ZT 23 and ZT 1 ($n = 3$ for each time point). The anterior segment, along with the neural retina, was dissected from the posterior segment that contains the RPE, choroid, and sclera. Following homogenization by sonicator, the isolated RPE cells were processed for RNA isolation with TRIzol (Ambion, 15596018) following the manufacturer's instructions. The total RNA was used to prepare 12 mRNA libraries following the standard Illumina protocol. Total RNA samples from the RPE were sent to Omega Bioservices (Norcross, GA, USA) for both library preparation and next-generation sequencing.

RNA-Seq Runs, Mapping and Estimation of Reads Per Kilobase Per Million

The 12 RNA-sequence (RNA-seq) libraries were then sequenced on the Illumina HiSeq2000 platform to produce approximately 65 million, 100 nucleotide paired-end reads per sample (reads 1 and 2). The reads were mapped to the University of California – Santa Cruz (UCSC; Santa Cruz, CA, USA) mouse genome assembly and transcript annotation (mm10). Mapping was performed with Bowtie2 (version 2.1.0) using the default settings. HTSeq-count (PyCharm Community Edition 2016.3.2) was used to generate counts of reads uniquely mapped to annotated genes using the UCSC mouse assembly mm10 gtf file. Further, reads per kilobase per million (RPKM) were calculated manually and only the genes having an RPKM of $\geq$1 were considered for further analysis.[21] Fold change was later calculated by using the RPKM values of the same gene at two different time points (ZT 1 versus ZT 23). Finally, we used *t*-test (paired-end = $\leq$0.05) and a cutoff of fold change $\geq$1.5 to determine the differentially expressed genes (DEGs).

To evaluate the significance of the identified DEGs, we used the Protein ANalysis THrough Evolutionary Relationships (PANTHER) Classification System and analysis tools to categorize DEGs by protein class, Gene Ontology (GO), Molecular Function, and GO Biological Process, and also to determine if any of these classes or GO terms were over-represented. First, differentially expressed genes with a fold change $\geq$2 were identified among the DEG's in each genotype and entered in the PANTHER database in increasing order of the *P* value. The PANTHER Overrepresentation Test (release 20171205) was used to search the data against the PANTHER database (PANTHER version 13.1, Released 2018-08-09) and the GO database (Release 20171205) to identify GO annotations and pathways over-represented in our data when compared to a reference mouse genome.

Western Blot

RPE samples were obtained from the eyes of control and KO mice at ZT 23, ZT 1, and ZT 3 using the methodology described in Baba et al., (2010) and then lysed in ice-cold RIPA buffer (50 mM Tris, pH 8.0; 150 mM NaCl; 1 mM EDTA; 1 mM EGTA; 1.0% Nonidet −40; and 1.0% sodium deoxycholate), 1x protease inhibitors, and 1x phosphatase inhibitor I and II. Following lysis and separation on

Investigative Ophthalmology & Visual Science

SDS/PAGE gel, the proteins were transferred to polyvinylidene fluoride (PVDF) membrane (Trans-Blot Turbo transfer system; Biorad Laboratories, Hercules, CA, USA; #1704156). The blot was incubated overnight at 4°C with Phospho-FAK (Tyr 397; 1:1000; Cell Signaling, Danvers, MA, USA; #3283), FAK (Cell Signaling; #3285). RPE-65 (1:2500, generous gift of T.M. Redmond, NEI). RPE-65 was used as a loading control for the amount of RPE protein present in the samples. Then, they were incubated with anti-rabbit horseradish peroxide (HRP; 1: 10000; Cell Signaling; #7074S) and developed. Band intensities were quantified by densitometry using Image J (1.51w).

Rac1 G-LISA

To analyse the activation of Rac1 in D_2R and WT RPE, G-LISA Rac1 activation assay Biochem Kit (Cytoskeleton, Inc., Denver, CO, USA) was used. Rac1 activation assay was performed following the manufacturer's instructions on fresh lysates of RPE tissue collected at ZT 23, ZT 1, and ZT 3, as mentioned previously (Baba et al., 2010).

Quantitative real-time- PCR

RPE samples were collected at ZT 23 and ZT 1 and subjected to RNA extraction using Trizol (Thermo Fisher Scientific; #15596026). Quantitative-PCR was performed using the CFX96 Touch Real-Time PCR Detection System (Bio-Rad Laboratories, Hercules, CA, USA) using iQ SYBR Green Supermix (Bio-Rad Laboratories Hercules; #1708880). All data for individual genes were normalized to 18S, according to a previously published protocol.[22]

Spectral Domain Optical Coherence Tomography

A Micron IV spectral domain optical coherence tomography (SD-OCT) system and a fundus camera were used (Phoenix Research Labs, Pleasanton, CA, USA) to analyze retinal morphology in the WT and D_2R KO mice at 3 and 12 months of age. Image-guided optical coherence tomography (OCT) images were obtained for the left and right eyes after a sharp and clear image of the fundus (with the optic nerve centered) was obtained. SD-OCT was a circular scan about 100 µm from the optic nerve head. Fifty scans were averaged. The retinal layers (indicated on the figure images) were identified according to published nomenclature. Total retinal thickness and thickness of the individual retinal layers were analyzed by using NIH Image J (1.51w).

ERG

Mice were subjected to dark adaptation for at least 1 hour and anesthetized with ketamine (80 mg/kg) and xylazine (16 mg/kg). The pupils were dilated with 1% atropine and 2.5% phenylephrine (Sigma, St. Louis, MO, USA). Mice were placed on a regulated heating pad set at 37°C with feedback from the rectal temperature probe. The eye was lubricated with the saline solution, and a contact lens type electrode (LKC Technologies; model: N1530NNC) was topically applied on the cornea. A needle reference was inserted in another side of the cheek, and the ground needle was inserted into the base of the tail. All preparation of ERG recordings was conducted under dim red light (<3 lux, 15W Kodak safe lamp filter 1A; Eastman Kodak, Rochester, NY, USA).

All electrodes were connected to a Universal DC Amplifier (LKC Technologies; model UBA-4200) and the signal was filtered from 0.3 to 500 hertz (Hz). Data were recorded and analyzed by EM for Windows (version 8.2.1; LKC Technologies). In the dark-adapted (scotopic) ERG protocol, seven series of flash intensity between 0.03 and 6.28 cd*s/m^2 were presented to the mouse eye. Flashes were generated by 530-nm green LEDs in a Ganzfeld illuminator (LKC Technologies), and intervals of flashes increased from 0.612 to 30 seconds as the intensity of the flashes increased. Responses of 3 to 10 flashes were averaged to generate a waveform for each step of light intensity, and a-wave and b-wave of ERG measurements were analyzed from the trace of waveforms.[23]

To measure the light-adapted (photopic) ERG, mice were placed in a Ganzfeld illuminator and cone-associated activity was isolated by saturating rods with 63 cd*s/m^2 of steady white background light. The four series of consecutive 10 white flashes (79.06 candela [cd]*s/m^2) were introduced at 2.5 minutes, 5 minutes, 10 minutes, and 15 minutes during the background light exposure. The background light was left on for 15 minutes while photopic ERGs records were measured. The traces of the ERG were averaged and stored on a computer for later analysis. The amplitude of the b-wave was measured from the trough of the a-wave to the peak of the b-wave or, if no a-wave was present, from the baseline to the b-wave peak. The spectral composition and irradiance of the light was monitored by a radio-spectrophotometer (USB 2000; Ocean Optics, Dunedin, FL, USA).

RPE Morphological Analysis

WT and D_2R KO mice were euthanized using cervical dislocation; the eyes were collected and then placed in Z-fix (Anatech; #170) for 10 minutes at room temperature and then were rapidly rinsed with 0.1 M PBS five times. Then RPE flat mounts were prepared as previously described.[24] Briefly, each eye was placed on a clean microscope slide (VWR, Suwanee, GA, USA; #16004-406) and any excess muscle or fat surrounding the eye was removed with spring scissors (WPI, Worcester, MA, USA; #501235). A single puncture was made in the middle of the cornea with Dumont #5 fine forceps (FST, Foster, CA, USA; #11254-20). By using Dumont #5/45 (FST; Foster, CA, USA; #11251-35) to support the eye globe, spring scissors were inserted into the initial puncture in the cornea and four radial cuts were made toward the dorsal end of the eye to where the optic nerve was located. The eyecup was then open and the lens was removed from the center of the eye. Next, the iris and the attached cornea was removed from the anterior ends of the petals. The retina was then removed to expose the underlying RPE. If necessary, center cuts in a petal were made to reduce the overall tensile stress of the RPE sheet.

Flat mounts were then incubated in a 1% BSA (Tocris Biosciences, Minneapolis, MN, USA; #5217) blocking solution for 30 minutes at room temperature. The blocking solution was removed, and the flat mounts were incubated overnight in Zonula occludens-1 (ZO-1) antibody (1:500; Millipore Sigma, Burlington, MA, USA; #MABT11) solution diluted in 1% BSA blocking solution at 4°C. On the next day, flat mounts were washed in a 1x Hank's Buffered Salt Solution (Gibco, Gaithersburg, MD, USA; #14065-056) with 0.1% Tween-20 (BioRad Laboratories, Hercules, CA, USA; #170-6531) for 5 times at 2 minutes each. Then the flat mounts were incubated in secondary antibody conjugated with Alexa Fluor 488 (1:500; goat anti-rat; Invitrogen, Carlsbad, CA, USA; #A11006) for 3 hours at room temperature on a shaker. Flat mounts were washed in the previously mentioned wash solution for 5 times at 2 minutes each. Under a dissecting microscope, the flat mounts were

Investigative Ophthalmology & Visual Science

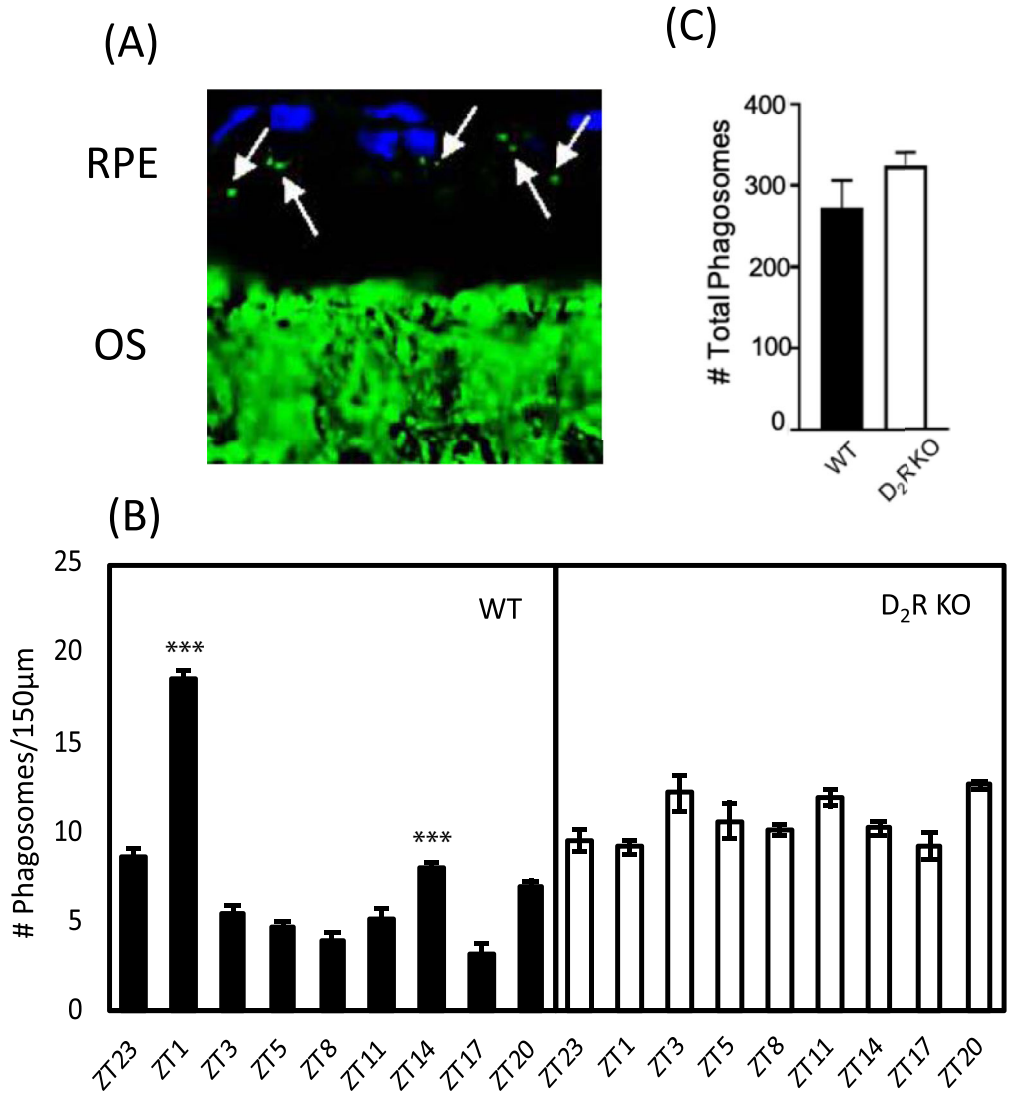

Figure 1. D_2R KO mice lack the burst of phagocytic activity after light onset. (A) Representative microphotograph of the mouse retinal section immunostained with anti-rhodopsin antibody (Rho4D2, green) and DAPI (blue). Phagosomes (marked with white arrows) can be seen as small particles present in RPE co-stained for rhodopsin and DAPI. (B) Bar graph indicating the number of phagosomes/150 µm of RPE at different time points. WT mice showed a significant increase in phagocytic activity at ZT 1 (1-way ANOVA, followed by post hoc Tukey test; ***P <0.001) and ZT 14 (1-way ANOVA, followed by post hoc Tukey test; ***P <0.001) compared to other time points. No increase in the number of phagosomes was observed in D_2R KO at ZT1 (two-way ANOVA, $p > 0.05$). (C) The total number of phagosomes during the different time points was not different in D_2R KO in comparison to WT (t-test; $P > 0.05$). RPE: retinal pigBars represent means ± SEM ($N = 4$–6). OS, outer segment.

flattened onto slides and mounted with Vectashield antifade mounting medium (Vector Laboratories, Burlingame, CA, USA; #H-1000) and allowed to dry at room temperature overnight. ZO-1 signal in the flat mount was visualized using a confocal microscope (Zeiss LSM 700) with two to three images of the peripheral region and four to six images from the central region captured from each petal of the flat mount. Images were then processed in CellProfiler (version 2.2.0) to determine the RPE morphological features such as area, eccentricity, compactness, and solidity.[24]

Statistical Analysis

In all cases, the data were tested for normal distribution using the Shapiro–Wilk test and equal variance was tested using the Brown–Forsythe test to check the fulfillment of the requirements for the parametric tests. Data were analyzed with t-test, one-way or two-way ANOVA. Post hoc multiple comparisons of interactions were performed with Tukey's test. Significance level was set at $P < 0.05$. Data are expressed as the mean ± standard error of the mean.

Results

Lack of D_2R Signaling Abolishes the Daily Burst in Phagocytic Activity by the RPE

Quantification of the phagosomes in the retinal sections at different time points in WT and D_2R KO mice (Fig. 1) revealed that in WT mice, the number of phagosomes in the

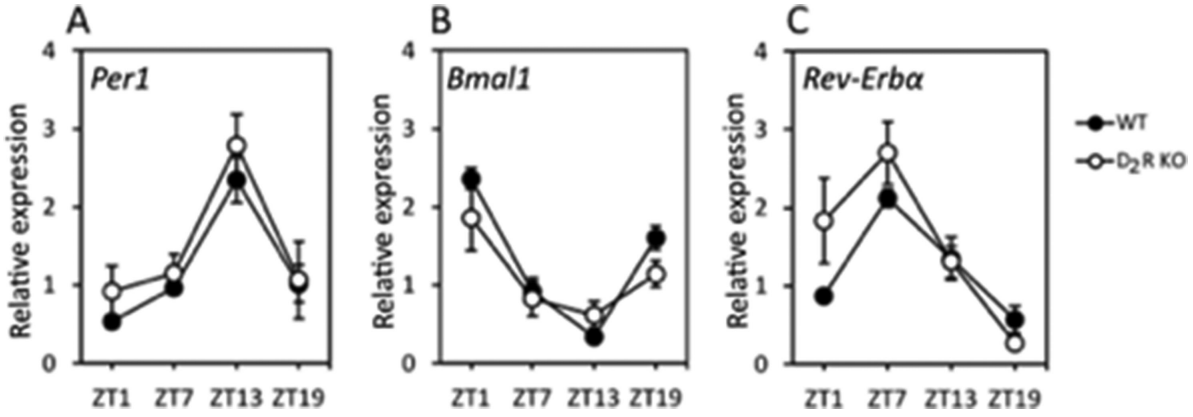

Figure 2. Removal of D_2R signaling does not affect the expression of the clock genes. *Per1* (A), *Bmal1* (B) and *Rev-Erbα* (C) mRNA expression levels, rhythmic pattern, and phase were not affected by the removal of the D_2R (2-way ANOVA, $P > 0.05$). Circles represent the means ± SEM ($P < 0.05$; $N = 4–6$).

RPE start to increase significantly at ZT 20 (1-way ANOVA, followed by Tukey test, Z17 versus ZT 20, $P < 0.001$) and peaked at ZT1 (1-way ANOVA, followed by Tukey test; ZT 20 vs. ZT 23, $P < 0.001$) and ZT 23 vs. ZT 1 ($P < 0.001$). The number of phagosomes then declined to basal level at other time points (1-way ANOVA, followed by Tukey test; ZT 1 vs. ZT 3, $P < 0.001$; ZT 1 vs. ZT 5, $P < 0.001$; ZT 1 vs. ZT 8, $P < 0.001$; ZT 1 vs. ZT 11, $P < 0.001$; ZT 1 vs. ZT 14, $P < 0.001$; ZT 1 vs. ZT 17, $P < 0.001$; ZT 1 vs. ZT 20, $P < 0.001$). A smaller peak in phagocytic activity was also observed at ZT 14 (1-way ANOVA, followed by Tukey test; ZT 3 vs. ZT 14, $P < 0.001$; ZT 5 vs. ZT 14, $P < 0.001$; ZT 8 vs. ZT 14, $P < 0.001$). However, this rise in number of phagosomes at ZT 14 was significantly smaller than that observed at ZT 1 (1-way ANOVA, followed by Tukey test, $P < 0.001$). In D_2R KO RPE, although we observed some significant differences in the number of phagosome at the different time points, no clear rhythmicity was observed. Finally, although in D_2R KO RPE an overall increase in phagocytic activity was observed, the total number of phagosomes during the day did not differ betweeen WT and D_2R KO RPE (*t*-test; $P > 0.05$).

Removal of D_2R Signaling Does not Affect the Expression of Clock Genes in the RPE In Vivo

Expression levels of mRNA in the RPE over the course of the day for three canonical clock genes (*Per1*, *Bmal1*, and *Rev-Erbα*) was analyzed by Q-PCR (Fig. 2). In both genotypes, the three clock genes showed a rhythmic pattern and no differences in the expression levels or phase were observed between WT and D_2R KO mice ($n = 5–6$; 2-way ANOVA, $P > 0.05$ in all cases).

RNA-Seq Analysis of the RPE Reveals Differentially Expressed Genes Between Time Points in WT and D_2R KO Mice

To identify DEGs between the different time points (ZT 23 vs. ZT 1) and genotypes, we used a cutoff expression of 1 RPKM, equivalent to one transcript per cell. A total of 13,387 and 12,487 protein-coding gene transcripts were detected in the RPE of WT and D_2R KO RPE, respectively, between the two time points (ZT 23 and ZT 1; Table). We also observed a higher number of DEGs in D_2R KO mice (1054 genes) than in WT (394 genes) between ZT 1 and ZT 23 ($P \leq 0.05$). Interestingly, only a small number (39) of DEGs overlapped between the two genotypes and although most (36) of the genes showed a common pattern, three genes were upregulated in one genotype and downregulated in the other (Table). Full details of the differential expression analysis can be found in Supplementary Table S1 and Table S2 and the biological process in which DEGs are involved at the two different time points and in the two genotypes are listed in Figure 3.

Table. Summary of the Gene Expression Profile in the RPE of WT and D_2R KO Mice Between ZT 23 and ZT 1 Time Points

	WT	D_2R KO
Total transcripts (>1 RPKM)	13,387	12,478
Differentially expressed transcripts	394	1054
Upregulated	247	651
Downregulated	147	403
Fold change >2	183	854
Fold change >=1.5 = <2	211	200

Although the total number of transcripts were not different between two genotypes, the number of DEGs were higher in the RPE of the D_2R KO mouse than in WT.

Integrin Pathway is Dysregulated in D2R KO Mice

GO analysis indicated the involvement of multiple signaling pathways that were upregulated or downregulated in the two genotypes (Figs. 4A, 4B). In WT mice, the integrin signaling pathway was upregulated at ZT 1, whereas in D_2R KO mice, this signaling pathway was downregulated. Further analysis of the genes associated with the integrin signaling pathway revealed significant differences in expression of these genes. In WT mice, Rap guanine exchange factor 1 (*Rapgef1*), Jun proto-oncogene (*Jun*), myosin light chain, phosphorylatable, fast skeletal muscle (*Mylpf*), and Fyn proto-oncogene (*Fyn*), and phosphatidylinositol-4,5-bisphosphate 3-kinase (*Pi3K*) were upregulated at ZT 1, whereas most of these genes were downregulated in D_2R KO (Figs. 4C, 4D). Genes like *Itgb5* and *Gsk3b* that were not differentially expressed in WT were downregulated (more than 2-fold) in D_2R KO mice (Figs. 4C, 4D).

Investigative Ophthalmology & Visual Science

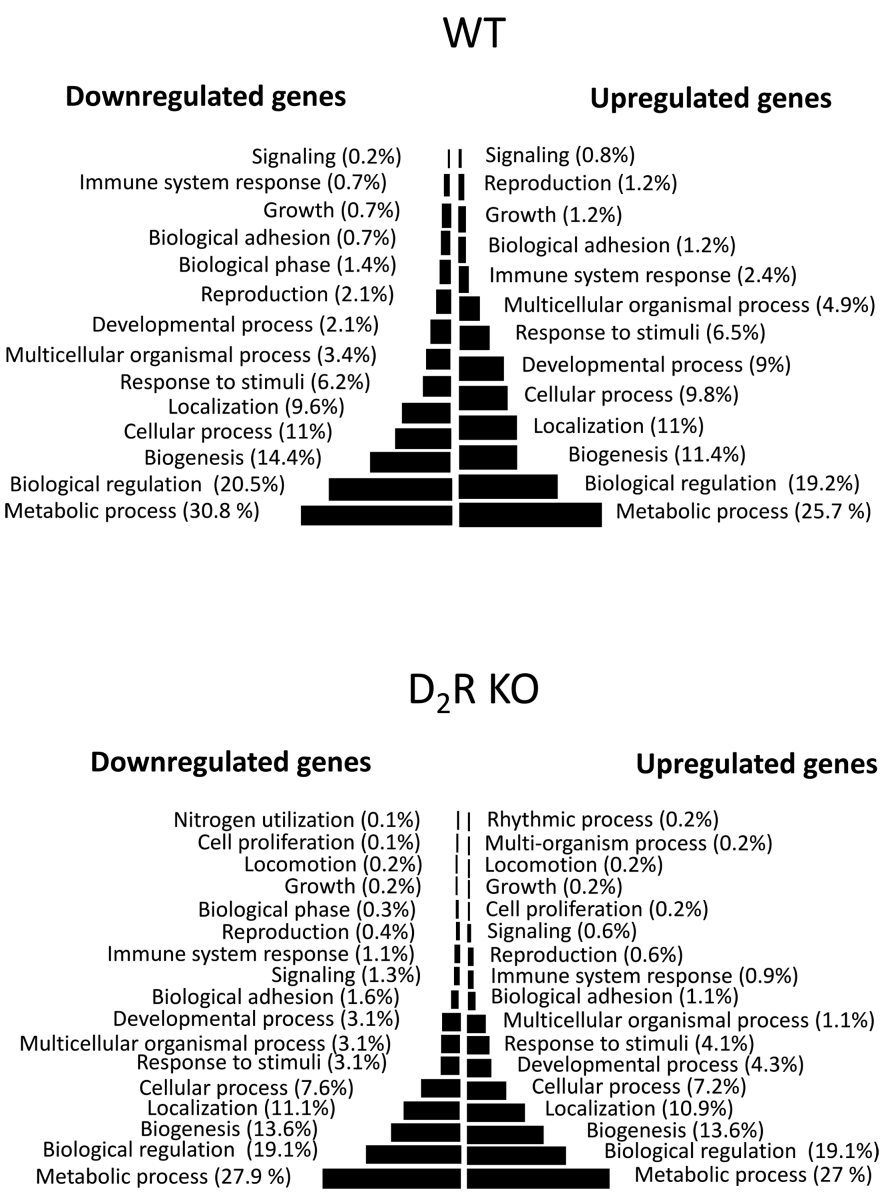

Figure 3. Gene ontology analysis and gene set enrichment in WT and D_2R KO mouse RPE at ZT 23 vs. ZT 1. The figure shows the biological processes that are upregulated and downregulated after the onset of light in WT and D_2R KOs. In both genotypes, the onset of light induced an upregulation of metabolic process, biological regulation, and biogenesis.

Removal of D_2R Inhibits the Activation of FAK and Rac1 After the Onset of Light

FAK and Rac1 have been shown to play a crucial role in phagocytic activity in RPE.[4,7] Western blot analysis indicated that the level of FAK phosphorylation at Tyr397 (p-FAK) in WT mice was increased at ZT 1 with respect to the values observed at ZT 23 and ZT 3 whereas no change in p-FAK levels was observed in D_2R KO mice at ZT 23, ZT 1, and ZT 3 (Fig. 5A). Densitometry analysis of the Western blot data confirmed that p-FAK level was significantly lower at ZT 1 in D_2R KO. In addition, no other difference was detected between the two genotypes at the other time points (Fig. 5B, 2-way ANOVA followed by Tukey test). Total FAK levels remained constant and were the same in both the genotypes (2-way ANOVA, $P > 0.05$). The levels of activated Rac1 indicated that at ZT 1, GTP-Rac1 levels were significantly increased in both genotypes with respect to the values observed at ZT 23 and ZT 3 (Fig. 5C; 2-way ANOVA followed by Tukey test, $P < 0.001$).

D_2R KO Mice do not Show any Changes in Retinal Morphology or ERG Responses

Fundus imaging did not show any significant difference between WT and D_2R KO mice at 3 and 12 months of age (Fig. 6A). Total retinal thickness was not different between WT and D_2R KO mice at 3 months (161.40 ± 2.40 µm vs. 168.44.02 ± 14.12 µm, $n = 4$–6; t-test, $P > 0.05$, Figs. 6B, 6C, 6D) or 12 months of age (163.14.11 ± 3.75 µm vs. 170.74 ± 3.10 µm, $n = 4$–6; t-test, $P > 0.05$; Figs. 6B, 6E, 6F). At 12 months, both WT and D_2R KO mice displayed no reduction in the thickness of the different retinal layers in comparison

Investigative Ophthalmology & Visual Science

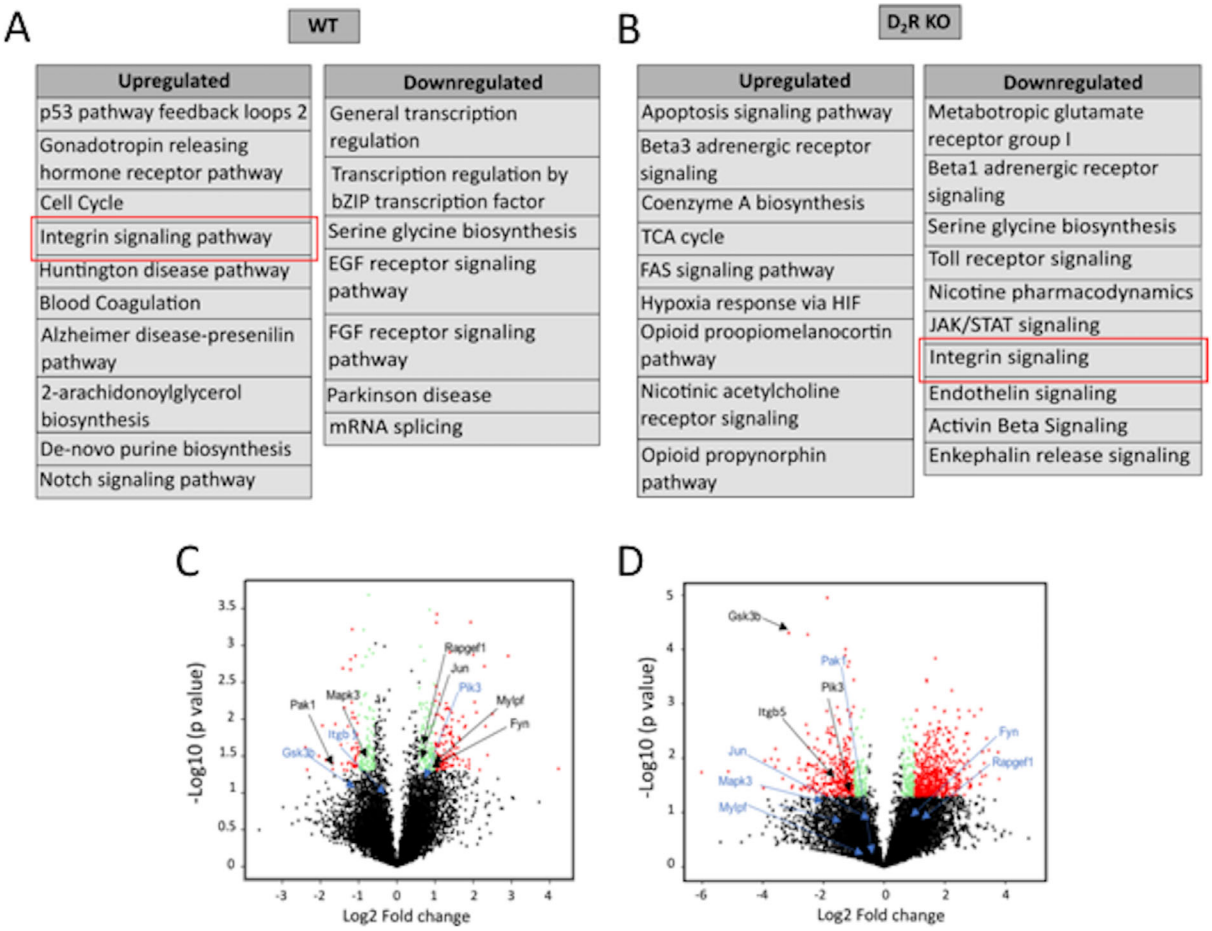

Figure 4. Pathway analysis of differentially expressed genes from WT and D_2R KO mouse RPE. (A, B) Differentially expressed genes having a fold change of >2 were analyzed in PANTHER to identify upregulated and downregulated pathways in both genotypes. Although integrin signaling (marked in the red box) was upregulated in WT, it was found to be downregulated in D_2R KO mouse RPE. (C, D) Volcano plot of transcript oscillations between ZT 23 and ZT 1 in WT and D_2R KO mouse RPE. The black dots indicate the nondifferentially expressed genes (fold change <1.5 and *P*- alue > 0.05). Green and red dots indicate the differentially expressed genes having a fold change >1.5 and 2, respectively, and a *P* value < 0.05. Also marked are the genes involved in integrin signaling; upregulated (black) and downregulated (blue).

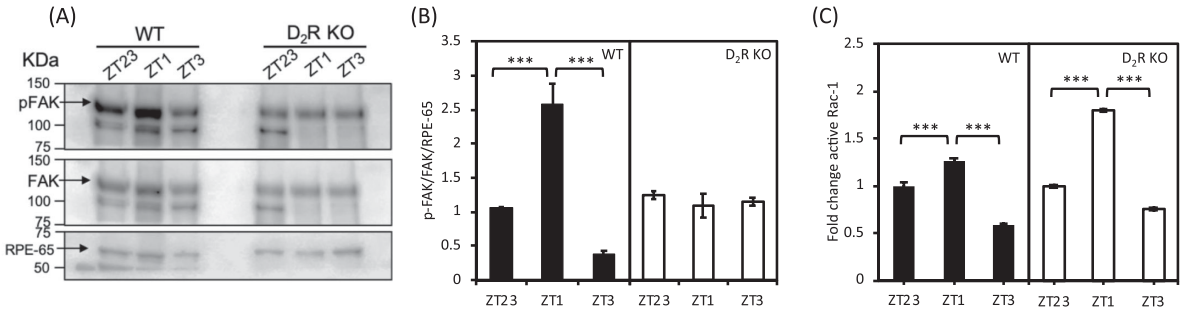

Figure 5. D_2R KO mice lack p-FAK increase after light onset. (A) Representative Western blot bands for RPE-65, FAK, and p-FAK in WT and D_2R KO mice at ZT 23, ZT 1, and ZT 3. Arrows indicate the specific 125 KDa band for p-FAK and FAK. An additional nonspecific band around 100 kD is also seen. A 65 KDa band is marked by an arrow for RPE-65 for the loading control. (B) Densitometry analysis of the bands intensity indicated a significant increase in p-FAK after the onset of light in WT (2-way ANOVA; ***$P < 0.001$), but not in D_2R KOs (2-way ANOVA; $P > 0.05$). Bars represent the means ± SEM (*$P < 0.001$). (C) Rac1 activity increased at ZT 1, both in WT (2-way ANOVA, followed by post hoc Tukey test; ***$P < 0.001$) and D_2R KO mice (2-way ANOVA; followed by post hoc Tukey test; ***$P < 0.001$, $N = 3$).

to their younger counterparts (*t*-test, $P > 0.05$ in all cases). Consistent with these results, we did not observe any significant difference between the two genotypes at both ages in the retinal functioning using scotopic and photopic ERG measurements (Figs. 7A–7D, 2-way ANOVA, $P > 0.05$).

D_2R Signaling Removal has no Effects on RPE Cell Morphology

Morphological analysis via CellProfiler (version 2.2.0) of the RPE using ZO-1 immunohistochemistry (Fig. 8A) revealed

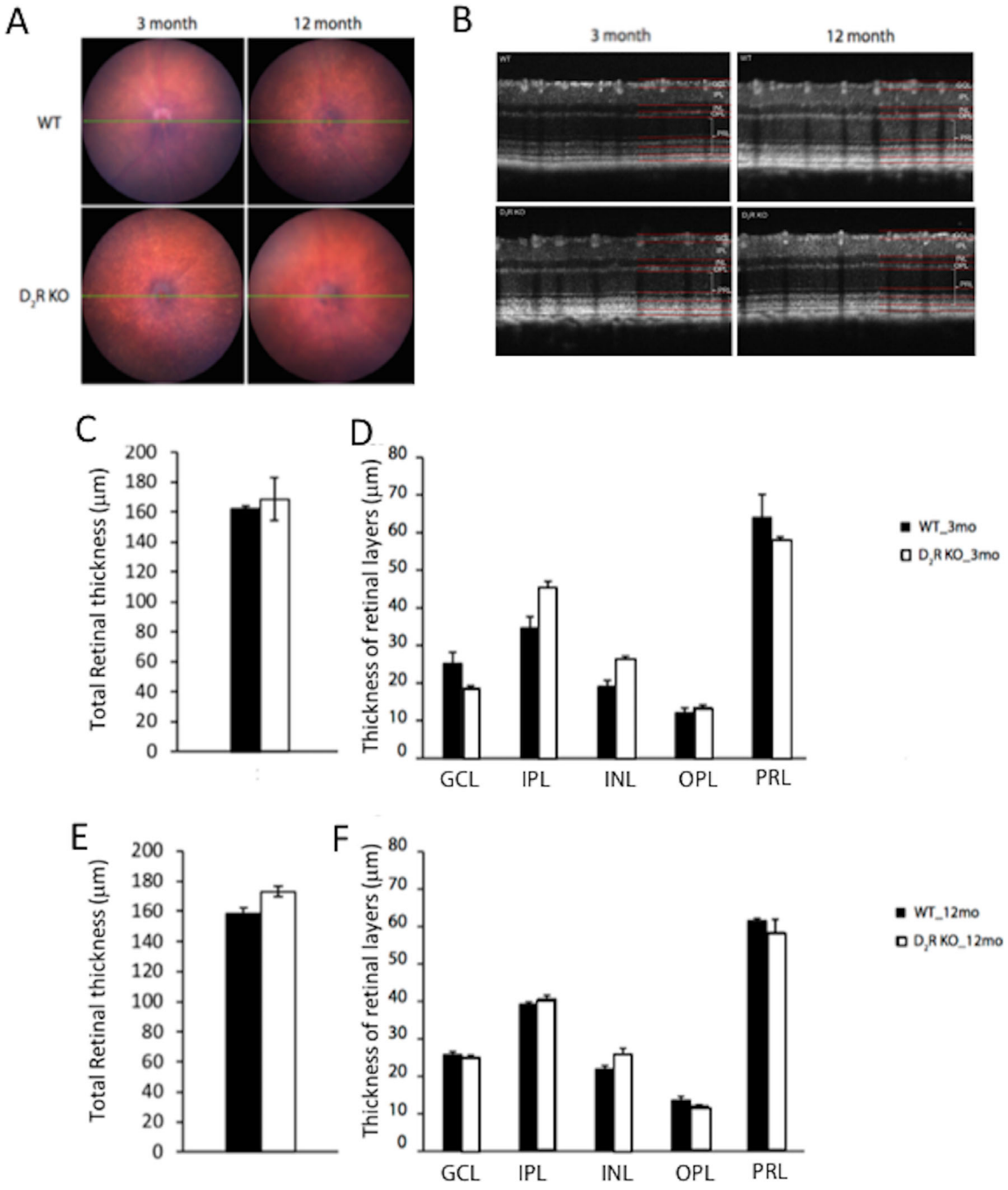

Figure 6. Retinal thickness is unaltered by the lack of D_2R signaling. (A) Fundus images acquired from WT and D_2R KO mice of 3 and 12 months of age did not show any significant difference between the two genotypes at both ages. (B) Total retinal thickness was not different between the two genotypes at both the age groups. (C, E). No differences were detected in the thickness of the different retinal layers between the two genotypes at both ages (D, F). We used *t*-tests, $P > 0.05$ in all cases. Bars represent the means ± SEM ($N = 4–6$). GCL, ganglion cells layer, INL, inner nuclear layer; IPL, inner plexiform layer; OPL, outer plexiform; PRL, photoreceptor layer).

no difference between the WT and D_2R KO mice RPE at 3 months of age in parameters like area, compactness, eccentricity, and solidity ($n = 5–6$; *t*-test, $P > 0.05$ in all cases, Figs. 8B–I). Further, in the 12-month-old group, we did not find any difference in the parameters mentioned above except for the area of RPE cells, which was increased in WT mice compared to D_2R KO mice (Fig. 8F, *t*-test, $P < 0.05$). In WT mice, the area was slightly but significantly increased in 12 month old with respect to 3 month old mice (*t*-test, $P < 0.05$), no other differences were observed between young and old WT mice (*t*-test, $P < 0.05$ in all cases). No differences in the parameters of the RPE morphology were observed between young and old in D_2R KO mice (*t*-test, $P > 0.05$ in all cases).

Discussion

The burst of phagocytic activity by the RPE after the onset of light has been described in several mammalian species[11–14,25] and, thus, many authors have proposed that

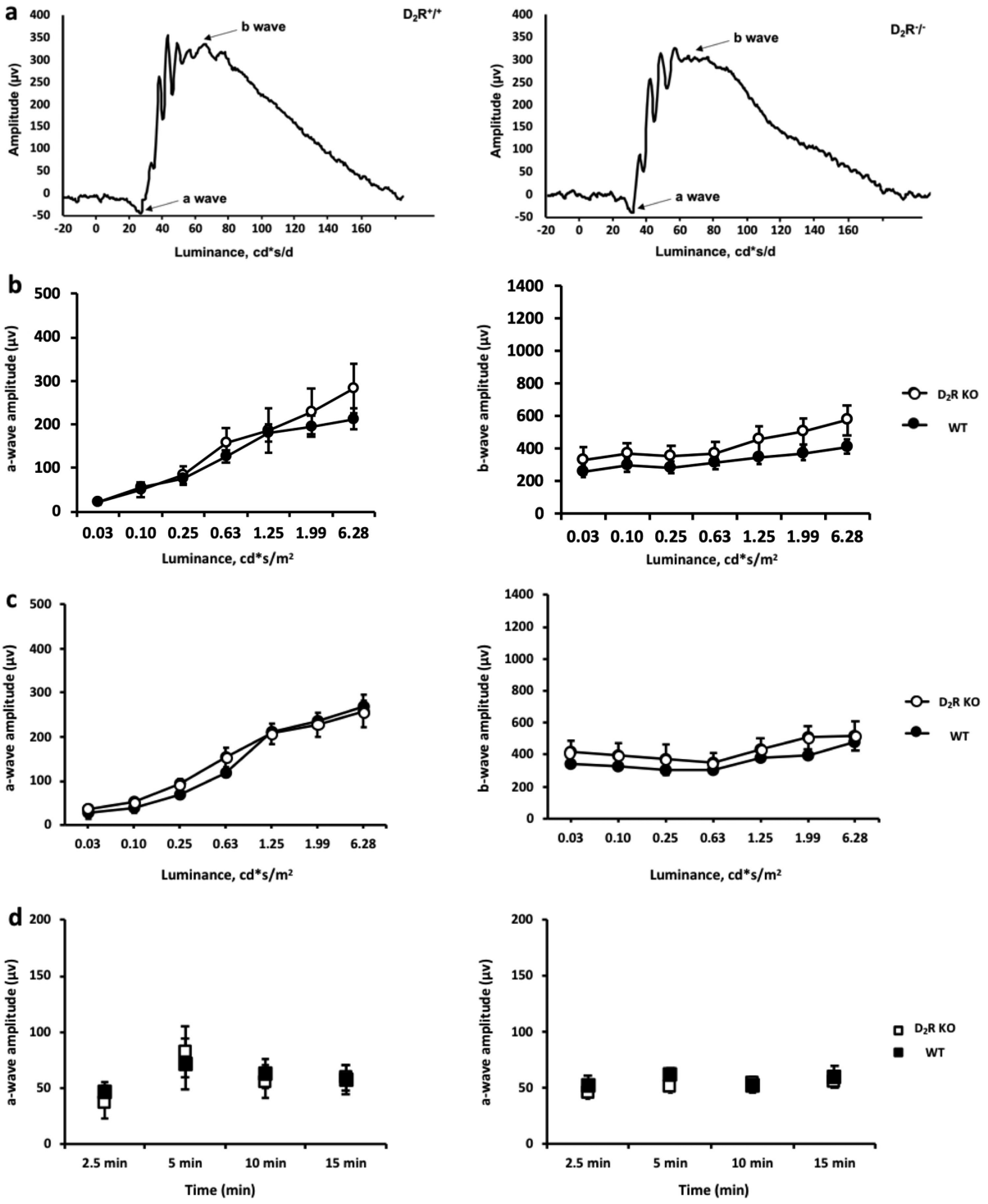

Figure 7. Lack of D_2R signaling does not affect the scotopic or photopic ERG responses. (A, B) The shape of the waveform in the scotopic ERG did not differ significantly between the WT and D_2R KO mice. (B, C) The a-wave and b-wave amplitudes of the scotopic ERGs did not differ between the genotypes both at 3 and 12 months of age. (D) No difference between in the photopic ERG were observed between the WT and D_2R KO mice at both ages (2-way ANOVA, $P > 0.1$). Circles and squares represent the means ± SEM ($N = 4$–6).

presence and the timing of the peak are vital for the correct processing of the POS.[26,27] Indeed, experimental data support this hypothesis because $\beta5^{-/-}$ mice, which lack the peak of the RPE phagocytic activity after the light onset, accumulate lipofuscin and have a reduced visual response during aging[4] even if the total daily phagocytic activity is not different between $\beta5^{-/-}$ and control mice.[4] An additional study has also reported that a small change in the timing of the peak (a phase-advance of about 3 hours) leads to lipofuscin accumulation.[15]

The data reported in this study show: (i) D_2R-deficiency completely abolished the burst in phagocytosis activity after

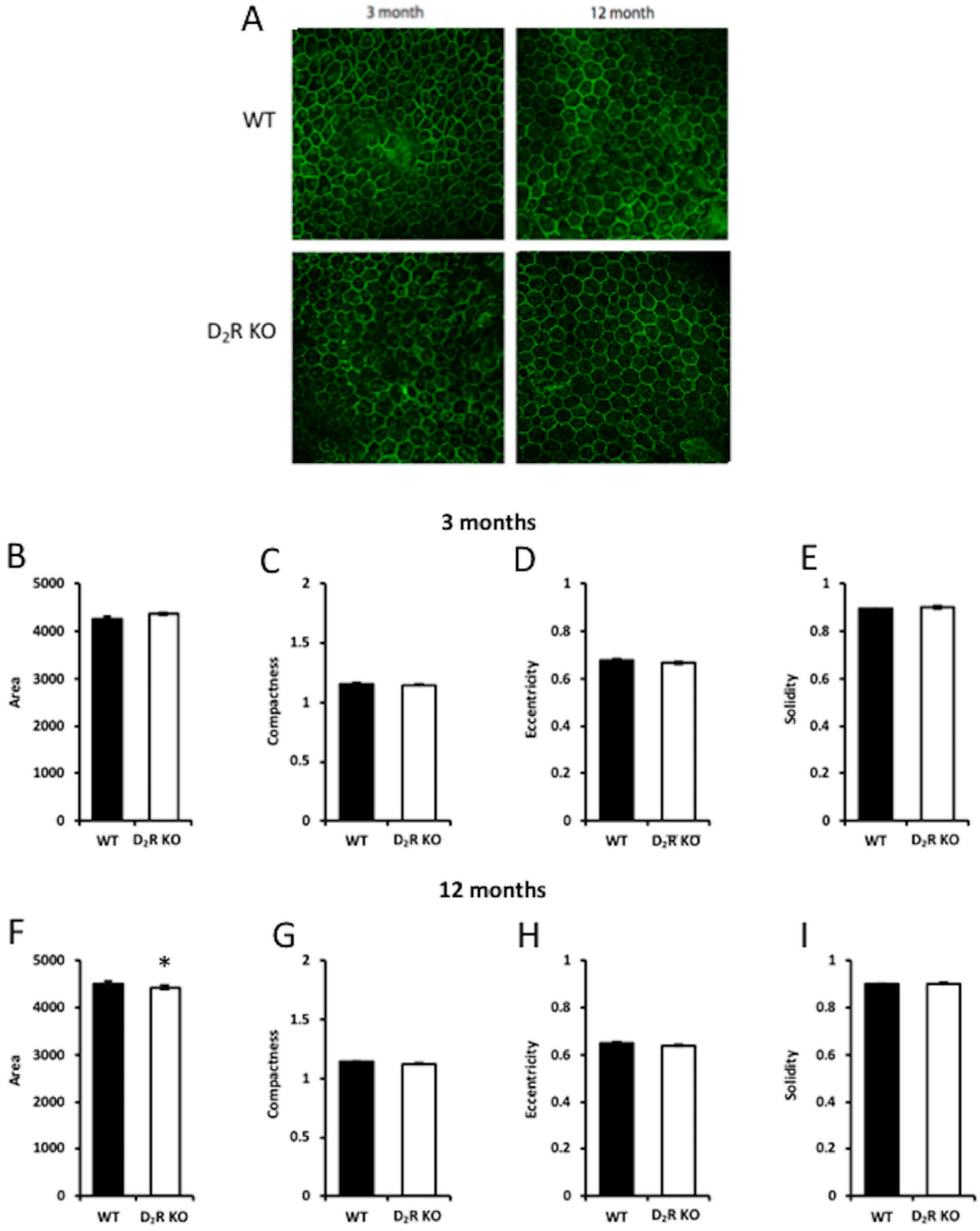

Figure 8. D_2R signaling does not affect RPE cell morphology. (A) Representative images of ZO-1 staining in WT and D_2R KO at 3 and 12 months. Analysis with CellProfiler (version 2.2.0) indicated that removal of D_2R signaling did not an affect the morphology of the RPE cells at 3 months of age (B–H) whereas at 12 months of age we observed a slight but significant difference in the total area of RPE cells between WT and D_2R KO mice (C; $P < 0.05$). Bars represent the means ± SEM ($N = 4–6$).

the onset of light; (ii) removal of D_2R signaling did not affect the expression of canonical clock genes in the RPE; (iii) analysis of the RPE transcriptome at ZT 23 and ZT 1 indicated a downregulation of the integrin signaling pathway in D_2R KO mice; and finally (iv) D_2R KO mice did not exhibit any sign of age-related morphological or functional abnormality in the retina. Thus, our data provide evidence that the absence in the burst of phagocytic activity in the early morning does not produce any obvious deleterious effect on the retina or RPE up to 1 year of age.

Investigative Ophthalmology & Visual Science

The fact that DA signaling plays such an essential role in the regulation of the burst of phagocytic activity is not surprising because DA is a key regulator of daily and circadian function within the retina,[28] and it is well known that DA synthesis and release is stimulated by light.[29,30] Similarly, it should not come as a surprise that D_2R—which are negatively coupled with adenyl cyclase and, thus, result in a decreased cAMP intracellular level—are involved in the activation of the peak of phagocytic activity by RPE cells because increases in intracellular cAMP decreases phagocytic activity whereas a decrease in cAMP is believed to stimulate phagocytic activity.[31] It is also important to mention that dopamine D_4 receptors do not mediate phagocytosis in the RPE because D_4R receptor KO mice still show a normal phagocytic activity after the onset of light[32] and activation of these receptors does not shift the RPE circadian clock.[20] D_1R and D_5R mRNAs are also present in the RPE,[20] but the role that these receptors play in the RPE biology is not yet known and, thus, additional studies are needed to fully understand the role that DA and its associated receptors play in the regulation of RPE biology.

As we have previously mentioned, several studies have shown that the rhythm in phagocytic activity is under control of the circadian clock[11,12] that is present in the RPE.[33,19,20,34] Therefore, it is quite surprising that we did not observe any effect on the daily pattern of clock genes expression in RPE in D_2R KO mice, thus suggesting that the RPE circadian clock may not be the primary driving mechanism in the signaling cascade controlling the burst in phagocytic activity.

Our RNA-seq data indicate that in both genotypes, a significant number of genes are differentially expressed before and after the onset of light and most of these genes (247) show a significant upregulation in both genotypes. Genes involved in metabolic and biological regulation were most affected and this is not unexpected since the transition from dark to light significantly affect cellular processes.

Using PANTHER, we also discovered that removal of the D_2R signaling has a significant effect on the genes involved in the integrin pathway, thus providing a possible mechanism by which D_2R signaling and integrin signaling interact to control the daily peak in phagocytic activity. In particular, the observation that *Itgb5* is dramatically downregulated in D_2R KO mice suggests that the mechanism that prevents the burst in the phagocytic activity after the onset of light is similar in the D_2R and $\beta5$ KO mice.

Our RNA-seq data also indicate an upregulation *Pi3K* signaling in WT, as reported by Mustafi et al.[8] However, it is essential to note that there are significant differences between our study and the one by Mustafi et al.[8] because, in their study, they compared the RPE transcriptome between 1.5 and 9.0 hours after the light onset, whereas we have compared the transcriptome 1 hour before and 1 hour after light onset and, thus, a direct comparison between our data set and Mustafi's data set is not possible.

Our data on FAK activation agree with the RNA-seq analysis and with previous studies[2,7] in which it was reported that activation of FAK signaling is required for the burst in phagocytic activity after the onset of light. Previous studies have also shown that Rac1 signaling is also involved in daily burst of phagocytic activity by the RPE,[7] although this pathway is activated by independent mechanisms and an inhibition of FAK did not prevent Rac1 activation.[7] Interestingly, in our study, we did not observe any major differences between the two genotypes with respect to the activation of Rac1 after light onset. Hence, our data suggest that removal of D_2R signaling only affects FAK activation this suggesting that Rac1 activation is not required for burst in phagocytic activity observed after light onset.

The observation that removal of the daily burst of the phagocytic activity did not produce any major adverse effects on the retina and RPE is somewhat surprising but not completely unexpected because mice lacking MGF-E8 (the ligand for $\alpha v\beta5$ integrin receptor) do not have a peak of phagocytic activity 1 to 2 hours after the onset of light[2] and do not show any decrease in scotopic ERG responses at least until 12 months old of age.[35] Although the Finnemann laboratory did not report on the RPE morphology, our data on the RPE morphology suggest that loss of D_2R signaling and the morning peak in the phagocytic activity do not produce a significant effect in young and old D_2R KO mice.

A recent study in which phagosome count was performed using electronmicroscopy to image the phagosomes has reported the presence in the mouse of a second peak at ZT 13.5 (i.e. 1.5 hours after the onset of dark).[36] Our study also detected a second peak in phagocytic activity at ZT 14 that was not present in D_2R KO. However, because we did not observe any difference in retinal functioning or RPE morphology between the D_2R and WT genotypes in young and in aged mice, we also suggest that the presence or absence of the morning and/or evening peak may not have any significant effect on the retina and RPE. The observation that the total number of phagosomes averaged throughout the day did not differ between D_2R and WT genotypes may explain this lack of pathology in the RPE and retina. Thus, the physiological role of the temporal regulation of POS phagocytosis remains unclear.

Altogether, these data suggest that the decrease in visual function and the increase in lipofuscin accumulation observed in $\beta5^{-/-}$ mice is not due to the lack of the phagocytic peak, but rather to other signaling pathways that $\alpha v\beta5$ integrin receptor may modulate. Further studies will be needed to address this critical question and to identify such pathways.

In conclusion, our data demonstrate that DA signaling - via D_2R - is responsible for the increase in RPE phagocytic activity after the onset of light. D_2R removal downregulates integrin signaling and thus FAK phosphorylation at ZT 1. Our data also indicate that the absence of the burst of phagocytic in the early morning does not produce any observable deleterious effects on the retina, at least until 12 months of age.

Acknowledgments

The authors thank Richard Huganir (Johns Hopkins University) for the generous gift of the D2K KO.

Supported by National Institutes of Health Grants: GM116760 (KB); R01EY026291 (GT); and 5U54NS083932 to Morehouse School of Medicine; R01EY004864, R01EY027711, and P30EY006360 (PMI); and an unrestricted departmental grant from Research to Prevent Blindness (Emory Department of Ophthalmology).

Disclosure: **V. Goyal**, None; **C. DeVera**, None; **V. Laurent**, None; **J. Sellers**, None; **M.A. Chrenek**, None; **D. Hicks**, None; **K. Baba**, None; **P.M. Iuvone**, None; **G. Tosini**, None

References

1. Young RW, Bok D. Participation of the retinal pigment epithelium in the rod outer segment renewal process. *J Cell Biol*. 1996;42:392–403.

2. Nandrot EF, Anand M, Almeida D, Atabai K, Sheppard D, Finnemann SC. Essential role for MFG-E8 as ligand for $\alpha v\beta 5$ integrin in diurnal retinal phagocytosis. *Proc Natl Acad Sci*. 2007;104:12005–12010.
3. Finnemann SC, Bonilha VL, Marmorstein AD, Rodriguez-Boulan E. Phagocytosis of rod outer segments by retinal pigment epithelial cells requires $\alpha v\beta 5$ integrin for binding but not for internalization. *Proc Natl Acad Sci*. 1997;94:12932–12937
4. Nandrot EF, Kim Y, Brodie SE, Huang X, Sheppard D, Finnemann SC. Loss of synchronized retinal phagocytosis and age-related blindness in mice lacking $\alpha v\beta 5$ integrin. *J Exp Med*. 2004;200:1539–1545.
5. Feng W, Yasumura D, Matthes MT, LaVail MM, Vollrath D. Mertk triggers uptake of photoreceptor outer segments during phagocytosis by cultured retinal pigment epithelial cells. *J Biol Chem*. 2002:277;17016–17022
6. Finnemann SC. Focal adhesion kinase signaling promotes phagocytosis of integrin-bound photoreceptors. *EMBO J*. 2003;22:4143–4154.
7. Mao Y, Finnemann SC. Essential diurnal Rac1 activation during retinal phagocytosis requires $\alpha v\beta 5$ integrin but not tyrosine kinases focal adhesion kinase or Mer tyrosine kinase. *Mol. Biol. Cell*. 2012;23:1104–1114.
8. Mustafi D, Kevany BM, Genoud C, Bai X, Palczewski. Photoreceptor phagocytosis is mediated by phosphoinositide signaling. *FASEB J*. 2012;27:4585–4595.
9. Bok D, Hall MO. The role of the pigment epithelium in the etiology of inherited retinal dystrophy in the rat. *J Cell Biol*. 1971;49:664–682.
10. Duncan JL, LaVail MM, Yasumura D, et al . An RCS-like retinal dystrophy phenotype in mer knockout mice. *Investigative Ophthalmology & Visual Science*. 2003;44:826–838.
11. La Vail MM. Survival of some photoreceptor cells in albino rats following long-term exposure to continuous light. *Invest Ophthalmol Vis Sci*. 1976;15:64–70.
12. Grace MS, Wang LA, Pickard GE, Besharse JC, Menaker M. Thetau mutation shortens the period of rhythmic photoreceptor outer segment disk shedding in the hamster. *Brain Res*. 1976;735:93–100.
13. Grace MS, Chiba A, Menaker M. Circadian control of photoreceptor outer segment membrane turnover in mice genetically incapable of melatonin synthesis. *Vis Neurosci*. 1999;16:909–918.
14. Bobu C, Hicks D. Regulation of retinal photoreceptor phagocytosis in a diurnal mammal by circadian clocks and ambient lighting. *Invest Ophthalmol Vis Sci*. 2009;50:3495–3502.
15. Laurent V, Sengupta A, Sánchez-Bretaño A, Hicks D, Tosini G. Melatonin signaling affects the timing in the daily rhythm of phagocytic activity by the retinal pigment epithelium. *Exp Eye Res*. 2017;165:90–95.
16. Ruggiero L, Connor MP, Chen J, Langen R, Finnemann SC. Diurnal, localized exposure of phosphatidylserine by rod outer segment tips in wild-type but not Itgb5−/− or Mfge8−/− mouse retina. *Proc Natl Acad Sci*. 2012;109:8145–8148
17. Reme C, Wirz-Justice A, Rhyner A, Hofmann S. Circadian rhythm in the light response of rat retinal disk-shedding and autophagy. *Brain Res*. 1986;369:356–360.
18. Mariani AP, Neff NH, Hadjiconstantinou M. 1-Methyl-4-phenyl-1, 2, 3, 6-tetrahydropyridine (MPTP) treatment decreases dopamine and increases lipofuscin in mouse retina. *Neurosci Lett*. 1986;7:221–226.
19. Baba K, Sengupta A, Tosini M, Contreras-Alcantara S, Tosini G. Circadian regulation of the PERIOD 2: LUCIFERASE bioluminescence rhythm in the mouse retinal pigment epithelium-choroid. *Mol Vis*. 2010;16:2605.
20. Baba K, DeBruyne JP, Tosini G. Dopamine 2 receptor activation entrains circadian clocks in mouse retinal pigment epithelium. *Sci Rep*. 2017;7:5103.
21. Mustafi D, Kevany BM, Bai X, et al . Evolutionarily conserved long intergenic non-coding RNAs in the eye. *Hum Mol Genet*. 2013;22:2992–3002.
22. Hiragaki S, Baba K, Coulson E, Kunst S, Spessert R, Tosini G. Melatonin signaling modulates clock genes expression in the mouse retina. *PLoS One*. 2014;9:e106819.
23. Marmor MF, Fulton AB, Holder GE, Miyake Y, Brigell M, Bach MI, International Society for Clinical Electrophysiology of Vision. ISCEV Standard for full-field clinical electroretinography (2008 update). *Doc Ophthalmol*. 2009;118:69–77.
24. Boatright JH, Dalal N, Chrenek MA, et al . Methodologies for analysis of patterning in the mouse RPE sheet. *Mol Vis*. 2015;2:40.
25. Teirstein PS, Goldman AI, O'Brien P. Evidence for both local and central regulation of rat rod outer segment disc shedding. *Invest Ophthalmol Vis Sci*. 1980;19:1268–1273.
26. Kevany BM, Palczewski K. Phagocytosis of retinal rod and cone photoreceptors. *Physiology*. 2010;25:8–15.
27. Sparrrow JR, Hicks D, Hamel CP. The retinal pigment epithelium in health and disease. *Curr Mol Med*. 2010;10:802–823.
28. McMahon DG, Iuvone PM, Tosini G. Circadian organization of the mammalian retina: from gene regulation to physiology and diseases. *Prog Retin Eye Res*. 2014;39:58–76.
29. Iuvone PM, Galli CL, Garrison-Gund CK, Neff NH. Light stimulates tyrosine hydroxylase activity and dopamine synthesis in retinal amacrine neurons. *Science*. 1978;202:901–902.
30. Brainard G, Morgan WW. Light-induced stimulation of retinal dopamine: a dose-response relationship. *Brain Res*. 1987;424:199–203.
31. Hall MO, Abrams TA, Mittag TW. The phagocytosis of rod outer segments is inhibited by drugs linked to cyclic adenosine monophosphate production. *Invest Ophthalmol Vis Sci*. 1993;34:2392–2401.
32. Nir I, Harrison JM, Haque R, et al . Dysfunctional light-evoked regulation of cAMP in photoreceptors and abnormal retinal adaptation in mice lacking dopamine D4 receptors. *J Neurosci*. 2002;22:2063–2073.
33. Terman JS, Reme CE, Terman M. Rod outer segment disk shedding in rats with lesions of the suprachiasmatic nucleus. *Brain Res*. 1993;605:256–264.
34. Ikarashi R, Akechi H, Kanda Y, et al . Regulation of molecular clock oscillations and phagocytic activity via muscarinic Ca 2+ signaling in human retinal pigment epithelial cells. *Sci Rep*. 2017;7:44175.
35. Nandrot EF, Finnemann SC. Lack of $\alpha v\beta 5$ integrin receptors or its ligand MFG-E8: distinct effects on retinal function. *Ophthalmic Res*. 2008;40:120–123.
36. Lewis TR, Kundinger SR, Link BA, Insinna C, Besharse JC. Kif17 phosphorylation regulates photoreceptor outer segment turnover. *BMC Cell Biol*. 2018;19:25.

Investigative Ophthalmology & Visual Science